Optical Properties of Human Skin in the NIR Wavelength Range of 1000-2200nm

Tamara L. Troy and Suresh N. Thennadil

Instrumentation Metrics, Inc.,
2085 Technology Circle Suite 302
Tempe, Arizona 85284

Phone: (480) 755-9483
Fax: (480) 755-9832

Abstract

In this paper we present the absorption coefficient, μ_a, and the isotropic scattering coefficient, μ'_s, for 22 human skin samples measured using a double integrating sphere apparatus in the wavelength range of 1000-2200nm. These *in vitro* results show that values for μ_a follow 70% of the absorption coefficient of water and values for μ'_s range from 3-16cm^{-1}. From the measured optical properties, it was found that a 2% Intralipid solution provides a suitable skin tissue phantom.

Keywords: tissue scattering, tissue absorption, near infrared optical properties

Introduction

Medical diagnostic and therapeutic techniques using light require knowledge of optical properties of tissue. In the past decade, significant research effort has gone into developing non-invasive measurement of blood glucose using near-infrared light.[1] While it is fairly straightforward to build calibrations for estimating glucose in simple systems like glucose-water, serum, etc., calibrations for non-invasive glucose estimation pose considerable challenges.[2-5] The difficulties arise due to the light being multiply scattered, the extent of which is dictated by the nature of the skin which varies dynamically due to changes in hydration and long term changes in thickness of the different layers of skin. To overcome the difficulties, an understanding of the interaction of light with skin is essential. In order to determine how light interacts with skin, the optical transport properties of absorption and scatter need to be determined. These properties aid in the design of a skin-instrument interface to optimally sample the tissue so as to maximize the glucose signal. In addition, they will help define the critical parameters used in constructing a reasonable skin tissue phantom (for example, made from a solution of Intralipid and water), which can serve as a model system for studying the problem of glucose estimation and other similar problems. Thus, the aim of this study was to obtain the optical properties of skin over the wavelength range of 1000-2200nm. By measuring different individuals and different sites, an estimate of the mean optical properties and the extent of variation about this mean over the wavelength range of interest can be obtained.

Skin is a heterogeneous medium made up of several distinct layers with spatially varying optical properties. Ideally, one would measure the optical properties of each layer. This task, however, is extremely complex since it would require separating and measuring layers of microscopic thickness. The measurements presented here represent lumped parameters for the absorption coefficient, μ_a, and the isotropic scattering coefficient, μ'_s, for the stratum corneum, the epidermis and the dermis.

Tissue optical property measurements in the near-infrared wavelengths are encumbered with difficulties owing to the necessity of extracting the tissues. It is important to keep in mind issues of sample freshness, blood drainage and tissue hydration. Maintaining tissue viability under measurement conditions is also a major concern. The major assumption in this work is that *in vitro* skin samples are a reasonable representation of the *in vivo* situation.

In this manuscript, we present *in vitro* values for the absorption coefficient, μ_a, and the isotropic scattering coefficient, μ'_s, for 22 skin samples collected from 14 subjects. The optical parameters measured in this study show how much μ_a, and μ'_s vary within a small population. In addition, Intralipid solutions of different concentrations were investigated to find the concentration that will best approximate the optical characteristics of skin in the wavelength region of 1100-2200nm.

Double Integrating Sphere Measurements of Tissue Optical Properties

A double integrating sphere system is a convenient tool to measure the optical properties of skin or any material of interest since it measures the diffuse reflectance, R_d, and the diffuse transmittance, T_d, simultaneously. Figure 1 illustrates the double integrating sphere (DIS) apparatus used to measure these parameters for the determination of the sample's optical properties (μ_a and μ'_s). It is not within the scope of this manuscript to go into detail about integrating sphere technology, and the reader is referred elsewhere.[6,7] The tissue sample is placed between two 15.2cm diameter integrating spheres (IS-060-IG, Labsphere, North Sutton, NH) which are coated with a diffusely reflective material suitable for this wavelength region. The entrance and exit ports on the spheres are 3.81cm in diameter. Internal baffles are located between the tissue sample and the detectors to prevent measurement of directly reflected or transmitted light.

Sample illumination between 1000-2200nm is achieved using a 100W tungsten halogen light source (OSRAM Co., Winchester, KY) coupled to a monochromator (slit width=2mm, N.A.=0.128, Instruments S.A., Inc. Edison, NJ). The bandwidth of the monochromator was 20nm with an average power of approximately 1mW. Two mirrors (ϕ=4in, f=406mm, Oriel Instruments, Stratford, CT) are used to re-image the exit slit from the monochromator onto the sample in order to achieve a reasonable spot size (nominal spot size was 2 x 5.6mm). The first mirror collimates the light leaving the monochromator exit slit and the second mirror focuses the light onto the sample. Each sphere contains both a 1.9μ InGaAs detector (ϕ=4mm, EG&G, Montgomeryville, PA) fitted with 1000nm filter (Cascade Optical Coatings, Santa Ana, CA) and a 2.6μ InGaAs

detector (ϕ=4mm, EG&G, Montgomeryville, PA) fitted with a 1300nm filter (Cascade Optical Coatings, Santa Ana, CA). The 1.9μ and 2.6μ detectors respectively, collect light between 1000-1660nm and 1660-2200 nm. Standard computer A/D acquisition records the detector signals.

From diffuse reflectance, R_d, and diffuse transmittance, T_d, values, the absorption and the isotropic scattering coefficients are obtained using the inverse adding-doubling program provided by Professor Scott Prahl at the Laser Research Center at St. Vincent Hospital, Portland Oregon.[8] This program is a numerical solution to the one speed radiative transport equation, which describes light propagation at steady state in a scattering medium.[6] The program is an iterative process, which estimates the reflectance and transmittance from a set of optical parameters until the calculated reflectance and transmittance match the measured values. Inputs that must be provided into the program are values for the anisotropy coefficient, g, and the refractive index, n, of the sample. Values for g and n are shown in Figure 2. In tissues, light is forward scattering and values for g used here range from 0.8 to 0.9 and come from data obtained by Roggan *et al.*[9] The refractive index is an important parameter because it describes the speed of light in tissue and it governs how the photons migrate. The refractive index, n, of skin is approximated from the refractive index of a 70/30 mixture of water and protein assuming that protein has a constant refractive index value of 1.5 over the entire wavelength region. The value for n of skin can be calculated using the following expression

$$n_{skin} = 0.7(A - B\lambda + C\lambda^2 - D\lambda^3 + E\lambda^4 - F\lambda^5) + 0.3 * 1.5 \qquad (1)$$

where A=1.58, B=8.45x10^{-4}, C=1.10x10^{-6}, D=7.19x10^{-10}, E=2.32x10^{-13}, F=2.98x10^{-17} and the wavelength, λ, is in nanometers. Values for A-F were obtained by fitting values of n for water[10,11] to a 5th order polynomial.

Validation of the Experimental Setup

Monodisperse polystyrene suspensions in water were used to validate the optical properties obtained from the double integrating sphere apparatus and the inverse adding-doubling algorithm. Because absorption is dominated by water in this wavelength region of 1000-2200nm, μ_a was determined from the electromagnetic properties of water (μ_a of polystyrene is negligible in this wavelength region due to its low absorbance and small concentration)

$$\mu_a = \frac{4\pi k}{\lambda}\phi_w . \qquad (2)$$

In Equation 2, k is the imaginary component of the refractive index of water,[10,11] λ is the wavelength of light, and ϕ_w is the volume fraction of water. The isotropic scattering coefficient, μ'_s was determined from the following linear relationship to the volume fraction of microsphere, ϕ_m

$$\mu'_s = (1-g)\frac{Q_{scat}\pi r^2}{4/3\pi r^3}\phi_m . \qquad (3)$$

The values for scattering efficiency, Q_{scat}, and the anisotropy coefficient, g, are calculated from the microsphere radius, r, and the refractive indices of polystyrene and water using Mie theory.[12] Figure 3 shows the typical agreement between theory and experimental

measurements for μ_a and μ'_s obtained from the integrating sphere apparatus. At wavelengths between approximately 1900 to 2050nm, the inverse adding-doubling program was not able to converge on acceptable values for μ_a and μ'_s. This lack of convergence occurred because the large absorbance due to the 1920nm-water band leads to insufficient amount of light reaching the detectors in either sphere. This decrease in signal can be illustrated by comparing μ_a of water at 1440nm and 1930nm, where μ_a is 32 and 125cm^{-1}, respectively. To examine the impact of this difference in absorption on light transport, consider the collimated transmission of light through a 1mm sample at two different μ_a values. Then,

$$\frac{I_2}{I_1} = \exp[-0.1(\mu_{a2} - \mu_{a1})] \quad (4)$$

where I_1 and I_2 represent the transmitted intensities at 1440 and 1930nm, respectively. Substituting the appropriate values for the corresponding absorption coefficients, it can be seen that the result is approximately a four-order magnitude decrease in the transmitted intensity and thus a tremendous reduction in the number of photon reaching the detector. Therefore, no experimental data will be reported in this region. The results conducted on polystyrene microspheres in water validate the experimental values for the μ_a and μ'_s measured by the apparatus from 1000-2200nm.

Tissue Specimen

Measurements were conducted on 22 skin samples collected from 14 subjects. Table I is a summary of the skin tissue demographics. The thicknesses for the stratum corneum, epidermis and dermis along with the comments section were determined from

histological examination. The samples were obtained from either Phoenix Regional Medical Center (Phoenix, AZ) or Scottsdale Healthcare (Scottsdale, AZ) with prior patient consent. The tissue samples were wrapped in saline soaked gauze, transported to Instrumentation Metrics, Inc. and measured within 24 hours of excision. All the skin samples were taken from tissue that would be otherwise destroyed following surgery. Human subject protocol guidelines of both hospitals were strictly followed and all procedures went through an Institutional Review Board approval.

After the skin samples were harvested from the patient, the subcutaneous fat was removed leaving an approximate 2mm-thick sample. All samples contained a stratum corneum, epidermis and dermis, which was determined from histology. The skin sample was usually large enough to cover the entire area of the sample port (2.5cm in diameter). For situations in which the sample was too small (samples 16-20), the sample ports were reduced to 1.3cm in diameter. Once at Instrumentation Metrics, Inc., the sample was placed between two glass plates and caliper measurements were taken to provide an accurate measurement of tissue sample thickness. The sample was then heated to 37°C at which time three measurements on each side of the sample were taken in order to account for any inhomogeneities in the sample. Measurements were conducted at body temperature conditions since it was previously shown that differences exist in the optical properties when measurements are taken at different temperatures.[13,14] It is also known that water absorption is highly sensitive to temperature in the near-infrared.[15] Experimental data was collected at a resolution of 20nm between 1000-1900nm and 2040-2200nm (a total of 52 wavelengths). Samples 1-6 were investigated with the 1.9μ InGaAs detectors fitted with 1100nm longpass filters permitting information from

1100nm onwards. The 1100nm filter was then changed to a 1000nm filter in order to collect data as low as 1000nm for subsequent samples.

The measured absorption coefficients, μ_a, for all 22 skin samples are found in Figure 4a. Also plotted here is the theoretical μ_a of 70% water since the concentration of water in tissue is approximately 60-80%. Because the major component of absorption in tissue is due to water, μ_a of skin is assumed to be similar to this value. Figure 4b is a plot of the isotropic scattering coefficient, μ'_s for all 22 samples along with theoretical data. For soft tissues Jacques[16] modeled the scattering coefficient as

$$\mu'_s(\lambda)=m(\lambda/\lambda_o)^{-1.5}. \quad (5)$$

In this equation, m is a constant ranging from $2x10^5$ to $2x10^6$ cm^{-1}, λ is the wavelength of light in nanometers and λ_o is a reference wavelength of 1nm. The experimental data for the skin samples shows that the values for μ'_s stay in the range of 3-16 cm^{-1} over the entire wavelength region and is better modeled using a value of m equal to $2x10^5$ cm^{-1}. Figure 4 nicely illustrates how the measured values of the optical properties follow the same trends.

The mean and inter-population standard deviations for the skin samples are plotted as a function of wavelength in Figure 5. All the data from the entire population studied here falls within 2.6 standard deviations for μ_a and 2.3 standard deviations for μ'_s. Table II lists the optical properties for all the samples at four selected wavelengths of 1000, 1460, 1600 and 2200nm. These wavelengths were chosen to include the endpoints (1000nm

and 2200nm), information near the 1450nm water band (large absorbance due to water) and the first overtone region (1600nm).

The availability of data from subjects of different ages allowed investigation into aging effects on the scattering and absorption coefficients of skin. The effect of aging on skin has been the topic of much research in the field of cosmetics. It is known that with age structural changes occur in skin.[17-21] One would expect these changes to be manifested in the scattering coefficients, in which case we would see a significant correlation between age and the scattering coefficients. To see if these changes are indicated by the data collected, the squared correlation coefficient r^2 was computed at each wavelength for μ_a and age and μ'_s and age. As can be seen from Figure 6 at a 95% significance level (indicated by the dotted line), age has negligible correlation with μ_a at all wavelengths and a significant correlation with μ'_s at wavelengths up to about 1800nm. This lack of correlation beyond 1800nm could be due to the lack of signal and higher noise in the measurement. Further, it was also found that the scattering coefficients were negatively correlated with age i.e. μ'_s decreased with increasing age. This negative correlation could be due to the reduction in density of cells.[21,22]

Skin Phantom Model

Intralipid is a fat emulsion that is typically used as a tissue simulating phantom in the therapeutic window (600-1000nm) since it has optical properties similar to tissue when its concentration is diluted to 0.5% fat by volume.[22,23] In this section solutions of

Intralipid were investigated in the wavelength region of 1000-2200nm in order to determine a concentration that has similar optical properties to skin.

As discussed above, the inverse adding-doubling program requires input values for the anisotropy coefficient, g, and the refractive index, n. The anisotropy coefficient was determined from Mie scattering theory[12] where the phospholipid micelle (particle size) was assumed to have a uniform diameter of 0.36μm. This value is the mean diameter of the Intralipid micelle measured by the manufacture (Fresenius Kabi Clayton R&D, Inc., Clayton, NC). The refractive index of Intralipid was calculated using a dispersion formula developed by Cauchy[22]

$$n(\lambda)=I+J/\lambda^2+K/\lambda^4. \quad (6)$$

In this equation I=1.451, J=1.154 x10^4 and K=-1.132 x10^9 and λ is in nanometers.

Because Intralipid is typically used as a nutritional supplement, the solution contains a small amount of glycerol (1.78% by volume). Glycerol has absorbance bands that are highly correlated to glucose absorbance bands.[24] Therefore, it is desirable to work with glycerol free solutions. In this study, the optical coefficients of 2, 5 and 10% Intralipid solutions were measured for both glycerol and glycerol free to determine if glycerol affects the scattering or absorption characteristics. The experimental results show that the optical properties of the two solutions (glycerol and glycerol free) are within experimental error (Figure 7).

In order to develop an Intralipid phantom with similar transport characteristics to skin, the right combination of μ_a and μ'_s needs to be determined. Although a 1.5% Intralipid solution matches the μ'_s of skin over entire wavelength region of 1000-2200nm (data not shown for brevity), μ_a is too high when compared to the concentration of water in tissue (approximately 60-80%). The major component of absorption in tissue is due to water and therefore, μ_a of skin is assumed to be similar to this concentration. Hence, the ratio of μ_a to μ'_s needed to be adjusted in order to obtain similar transport properties as skin. The similarity relations described by Flock *et al.* were used [23]

$$\frac{\mu'_{s,1}}{\mu_{a,1}} = \frac{\mu'_{s,2}}{\mu_{a,2}}. \qquad (7)$$

This equation predicts that two mediums will yield similar values for diffuse reflectance, R_d, when the above equation holds. The relationship was derived from the diffusion approximation (i.e. $\mu'_s >> \mu_a$) and therefore, is not exact in this wavelength region especially around the 1450nm and the 1920nm water bands. Figure 8 is a plot of μ'_s/μ_a for Intralipid concentrations ranging from 1% to 4% along with the minimum and maximum skin measurements. Experimentally measured data from the 2% Intralipid solution was used to calculate values for the other concentrations. At wavelengths less than 1900nm, a 2% Intralipid concentration will provide a reasonable tissue-simulating phantom. At wavelengths greater than 2100nm, an Intralipid solution between 2% and 4% will provide a reasonable tissue-simulating phantom. If only one concentration is practical, a 2% solution should provide the best correlation to skin over the entire wavelength region. This result is also corroborated by Hazen *et al*. who report that the

diffuse reflectance measurements of a 2% Intralipid solution have similar reflectance spectra to a non-invasive human arm measurement.[24]

Discussion

We found that the deviations in optical properties for human skin samples studied here are fairly small. The experimentally measured optical properties for our entire population fall within 2.6 standard deviations for μ_a and 2.3 standard deviations for μ'_s (Figure 5). In the wavelength range of 1000-2200nm, we found that values for μ'_s fall between 3-16cm^{-1}. These results show that the range of μ'_s for skin is much smaller than previously reported values for soft tissue.[16] Because soft tissue includes more than one tissue type, these results are reasonable since only skin was investigated here. The values for μ_a closely resemble 70% of water. It should also be noted that the skin samples were wrapped in saline soaked gauze, which may have affected the values for μ_a. From these measured optical properties, it was determined that Intralipid could be used as a skin tissue phantom over the wavelength range of 1000-2200nm provided a solution of approximately 2% is used. The results also reveal an inverse correlation between μ'_s and age from 1000-1800nm possibly due to the reduction of cell density with age. Although the data studied here come from a small population (22 samples from 14 subjects), the results can be used for sensitivity studies to aid in the developmental design of suitable interfaces for non-invasive measurements.

Acknowledgements

The authors wish to acknowledge the assistance of Holger Fuchs, Frank Grochocki and Glenn Kees for their improvements to the experimental design. We would like to thank Matthew Welch for preparing the Intralipid samples. Much appreciation goes to Ken Meissner for his helpful suggestions.

References

1. H.M. Heise, "Near-infrared spectrometry for in vivo glucose sensing," Chap. 3 in *Biosensors in the Body Continuous in vivo Monitori*ng, D.M. Fraser, Ed., pp. 79-116, John Wiley and Sons Ltd, West Sussex, England (1997).

2. S. Pan, H. Chung and M.A. Arnold, "Near-infrared spectroscopic measurements of physiological glucose levels in variable matrices of protein and triglycerides," *Anal. Chem*. **68,** 1124-1135 (1996).

3. H. Zeller, P. Novak, and R. Landgraf, "Blood glucose measurement by infrared spectroscopy," *International Journal of Artificial Organs* **12**, 129-135 (1989).

4. G.W. Small, M.A. Arnold and L. Marquardt, “Strategies for coupling digital filtering with partial least-squares regression: application to the determination of glucose in plasma by Fourier transforms near-infrared spectroscopy,” *Anal. Chem.* **65**, 3279-3289 (1993).

5. M.J. McShane, G.L. Cote and C. Spiegelman, “Variable selection in multivariate calibration of a spectroscopic glucose sensor,” *Applied spectroscopy* **51**, 1559-1564 (1997).
6. S.A. Prahl, M.J.C. van Gemert and A.J. Welch, “Determining the optical properties of turbid media by using the adding-doubling method,” *Applied Optics* **32**, 559-568 (1993).

7. J.W. Pickering, S.A. Prahl, N. van Wieringen, J.F. Beek, J. Sterenborg and M.J. van Gemert, “Double integrating sphere system for measuring the optical properties of tissue,” *Applied Optics* **32**, 399-410 (1993).

8. http://omlc.ogi.edu/software/iad/index.html

9. A. Roggan, J. Beuthan, S. Schrunder and G. Mueller, “Diagnostik und Therapie mit dem Laser,” *Physikalische Blaetter***55**, 25-30 (1999).

10. D. Segelstein, *The Complex Refractive Index of Water*, (masters thesis, University of Missouri, Kansas City, MO, 1981).

11. P. Ray, “Broadband complex refractive indices of ice and water,” *Applied Opt*ics **11**, 1836-1844 (1972).

12. C.F. Bohren and D.R. Huffman, *Absorption and Scattering of Light by Small Particles*, Wiley, New York (1983).

13. T.L. Troy, D.L. Page and E.M. Sevick-Muraca, “Optical properties of normal and diseased breast tissues: prognosis for optical mammography,” *Journal of Biomedical Optics* **1**, 342-355 (1996).

14. J. Laufer, R. Simpson, M. Kohl, and M. Cope, “Effect of temperature on the optical properties of *ex vivo* human dermis and subdermis,” *Phys. Med. Biol*. **43,** 2479-2489 (1998).

15. K.H. Hazen, M.A. Arnold and G.W. Small, “Temperature-Insensitive Near-Infrared spectroscopic measurements of glucose in aqueous solutions,” *Applied Spectroscopy* **48**, 447-483 (1994).

16. S.L. Jacques, “Origins of optical properties in the UVA, visible and NIR regions,” *Opt. Soc. Am.*, Topical Meeting, Orlando, Florida, March (1996).

17. C.H. Daly and G.F. Odland, “Age-related changes in the mechanical properties of human skin,” *Journal of Investigative Dermatology* **73**, 84-87 (1979).

18. G.L. Grove, R.M. Lavker, E. Hoelsle, and A.M. Kligman, “Use of nonintrusive tests to monitor age-associated changes in skin,” *J. Soc. Cosmet. Chem*., **32**, 15-26 (1981).

19. W. Andrew, R.H. Behnke, and T. Sato, “Changes with advancing age in the cell population of human dermis,” *Gerontologia*, **10**, 1-19 (1964).

20. T. Miyahara, A. Murai, T. Tanaka, S. Shiozawa and M. Kameyama, “Age related differences in human skin collagen: solubility in solvent, susceptibility to pepsin digestion, and the spectrum of solubilized polymeric collagen molecules,” *Journal of Gerontology* **37,** 651-655 (1982).

21. B.A. Gilchrest, “Aging of Skin,” Chap. 11, in *Dermatology in General Medicine*, Ed. T.B. Fitzpatrick, p146-152, McGraw-Hill, New York, NY (1993).

22. H.J. van Staveren, C.J.M. Moes, J. van Marie, S.A. Prahl and M.J.C. van Gemert, “Light scattering in Intralipid-10% in the wavelength range of 400-1100 nm,” *Applied Optics* **30**, 4507-4514 (1991).

23. S.T. Flock, S.L. Jacques, B.C. Wilson, W.M. Star and M.J.C. van Gemert, “Optical properties of Intralipid: a phantom medium for light propagation studies,” *Lasers in Surgery and Medicine* **12**, 510-519 (1992).

24. K.H. Hazen, J.M. Welch, T.L. Ructhi, A.D. Lorenz, and T.B. Blank, personal communications.

Table I: Demographic summary of the human skin samples along with microscopic evaluation.

Table II: Measured optical properties of human skin samples reported as the mean ± the standard deviation at wavelengths of 1000, 1460, 1500 and 2200nm. Samples 1-6 were investigated using 1100nm filters at the 1.9μ InGaAs detectors, therefore no information was collected at 1000nm. For the remaining samples, the 1100nm filters were switched to 1000nm filters in order to collect data over the wavelength range of 1000-2200nm.

Figure 1: Schematic of the double integrating sphere apparatus. The 1.9μ InGaAs detectors collect data from 1000-1660nm, and the 2.6μ InGaAs detectors collect data from 1660-2200nm.

Figure 2: The values for the anisotropy coefficient, g,[9] (solid line) and the refractive index, n,[10,11] (dashed line) of tissue as a function of wavelength used in this study.

Figure 3: The absorption coefficient, μ_a, and the isotropic scattering coefficient, μ'_s, of polystyrene microspheres in water over the wavelength region of 1000-2200nm. The particle diameters and volume fractions are (a) d=0.520μm and ϕ_m=0.01, (b) d=0.600μm and ϕ_m=0.0128 and (c) d=0.816μm and ϕ_m=0.0079. The solid lines represent that predicted by the electromagnetic theory (μ_a) or Mie Scattering Theory (μ'_s), and the symbols are the experimentally measured values. Data was taken every 20nm. Because the high degree of absorption between 1900-2050nm causes an inability to converge on reasonable values, no experimental data is reported in this region.

Figure 4: (a) Plot of the experimentally measured absorption coefficient, μ_a, for 22 human skin samples (solid lines) and the theoretical absorption coefficient, μ_a, for 70% water (dotted line). (b) Plot of the isotropic scattering coefficient, μ'_s, for 22 human skin samples for both experimental data (solid lines) and Equation 3 with m equal to $2x10^5$ or $2x10^6$ (dotted lines).

Figure 5: The average (solid line) (a) absorption coefficient, μ_a, and (b) isotropic scattering coefficient, μ'_s, plotted with population standard deviations (dotted lines) of 22 human skin samples taken from 14 subjects. The data from the entire population falls within 2.6 standard deviations for μ_a and 2.3 standard deviations for μ'_s.

Figure 6: The squared correlation coefficient, r^2, of (a) absorption with age, and (b) scattering with age (solid lines). Also included is the 95% significance level (dotted lines).

Figure 7: The (a) absorption coefficient, μ_a, and (b) isotropic scattering coefficient, μ'_s, as a function of wavelength for a 2% (solid line), 5% (dash-dot line) and 10% (dashed line) Intralipid solution and a 2% (solid line with symbol), 5% (dash-dot line with symbol) and 10% (dashed line with symbol) glycerol free Intralipid solution.

Figure 8: Plot of μ'_s/μ_a as a function of wavelength for Intralipid concentrations varying from 1% to 4% by volume along with the minimum and maximum skin measurements (solid lines). The inlayed graph shows a blow up of the 1600-2200nm region.

Table I

Subject	Sample	Age	Gender	Sample Location	Stratum Corneum (μm)	Epidermis (μm)	Dermis (μm)	Wavelength (nm)	Comments
01	01	51	F	Back of knee, left leg	40-70	40-150	300	1200-2200	Moderate inflammation in dermis
01	02	51	F	Back of knee, left leg	40-70	40-140	300	1200-2200	Moderate inflammation in dermis
02	03	66	F	Lower back, right side	20-50	30	200	1100-2200	Mild solar damage
02	04	66	F	Lower back, right side	20-50	30	200	1100-2200	Mild solar damage
03	05	67	F	Shin, right leg	20-50	30-50	200	1100-2200	Mild solar damage, chronic inflammation
03	06	67	F	Shin, right leg	20-50	30-50	200	1100-2200	Mild solar damage, chronic inflammation
04	07	64	M	Thigh, right leg	20-30	50-90	300	1000-2200	Mild chronic dermatitis
05	08	75	M	Lower thigh, left leg	8-12	20-60	200	1000-2200	Normal skin
05	09	75	M	Lower thigh, left leg	8-12	20-60	200	1000-2200	Normal skin
06	10	42	F	Groin, left side	5	25-30	200	1000-2200	Mild chronic inflammation
06	11	42	F	Groin, left side	5	25-30	200	1000-2200	Mild chronic inflammation
07	12	33	M	Posterior thigh, right side	2-5	5-10	300	1000-2200	Mild chronic dermatitis
08	13	52	F	Axillary, right side	5-7	25	100	1000-2200	Mild perivascular chronic inflammation
09	14	37	M	Back of thigh, upper left	3	13	300	1000-2200	Mild chronic dermatitis
10	15	70	M	Scalp	4-15	8-10	200	1000-2200	Mild chronic dermatitis w/ solar elastosis
11	16*	61	M	Scalp	2-4	6	300	1000-2200	Mild chronic dermatitis w/ solar elastosis
12	17*	68	F	Scalp/facial tissue	2	8-10	200	1000-2200	Mild solar damage, chronic inflammation,
12	18*	68	F	Scalp/facial tissue	2	8-10	150	1000-2200	Sever solar damage, mild chronic inflammation
13	19*	53	F	Scalp/facial tissue	4	10	200	1000-2200	Mild chronic inflammation
13	20*	53	F	Scalp/facial tissue	4	10	200	1000-2200	Mild solar damage
14	21	52	F	abdomen	4-5	10	200	1000-2200	Mild chronic inflammation
14	22	52	F	abdomen	4-5	10	200	1000-2200	Mild chronic inflammation

*Due to the small size of the sample, the 2.5cm diameter sample ports on the experimental set-up were reduced to 1.3cm for these measurements.

Table II

Subject	Sample	λ=1000nm						λ=1460nm						λ=1600nm						λ=2200nm					
		μ_a (cm^{-1})			μ'_s (cm^{-1})			μ_a (cm^{-1})			μ'_s (cm^{-1})			μ_a (cm^{-1})			μ'_s (cm^{-1})			μ_a (cm^{-1})			μ'_s (cm^{-1})		
		mean	±	std dev	mean	±	std dev	mean	±	std dev	mean	±	std dev	mean	±	std dev	mean	±	std dev	mean	±	std dev	mean	±	std dev
01	01	---	±	---	---	±	---	17.88	±	1.12	10.74	±	0.49	5.35	±	0.24	8.06	±	0.29	7.46	±	0.56	7.17	±	0.26
01	02	---	±	---	---	±	---	18.70	±	1.13	11.39	±	0.65	5.46	±	0.27	8.62	±	0.34	8.86	±	0.46	8.15	±	0.26
02	03	---	±	---	---	±	---	16.01	±	0.56	9.83	±	0.59	4.91	±	0.10	6.78	±	0.45	10.94	±	0.23	9.00	±	0.54
02	04	---	±	---	---	±	---	12.65	±	0.96	8.61	±	0.63	3.86	±	0.28	6.04	±	0.29	8.58	±	0.55	7.74	±	0.23
03	05	---	±	---	---	±	---	16.58	±	3.26	11.68	±	1.41	5.15	±	0.60	8.89	±	1.11	9.65	±	1.17	10.31	±	0.81
03	06	---	±	---	---	±	---	18.07	±	0.42	13.13	±	0.63	5.60	±	0.17	10.34	±	0.52	11.26	±	0.16	12.20	±	0.88
04	07	0.69	±	0.01	10.45	±	0.61	16.64	±	0.95	10.75	±	0.81	4.96	±	0.27	7.72	±	0.40	13.04	±	2.36	9.42	±	1.57
05	08	0.83	±	0.03	12.25	±	1.20	19.06	±	1.22	11.46	±	1.09	5.75	±	0.27	8.31	±	0.76	11.92	±	0.41	10.34	±	0.76
05	09	0.85	±	0.02	11.66	±	0.96	18.03	±	2.01	11.19	±	1.51	5.61	±	0.56	7.87	±	0.81	11.85	±	0.83	10.03	±	0.90
06	10	0.80	±	0.01	14.17	±	0.71	20.49	±	0.89	13.64	±	1.44	5.85	±	0.14	10.05	±	0.55	12.46	±	0.42	11.79	±	0.69
06	11	0.77	±	0.03	13.95	±	1.12	20.24	±	1.04	13.18	±	1.72	5.76	±	0.28	9.48	±	0.91	12.71	±	0.58	10.89	±	1.20
07	12	0.82	±	0.02	14.35	±	0.81	19.01	±	1.28	13.30	±	0.91	5.81	±	0.33	10.14	±	0.49	11.13	±	1.21	9.00	±	0.33
08	13	0.97	±	0.08	13.70	±	0.35	21.39	±	1.25	12.54	±	0.72	6.17	±	0.30	9.94	±	0.78	12.53	±	0.84	9.45	±	0.84
09	14	0.82	±	0.02	15.00	±	0.49	23.31	±	0.71	12.32	±	0.51	6.68	±	0.11	10.01	±	0.37	15.19	±	1.37	8.54	±	0.52
10	15	1.04	±	0.02	12.26	±	0.44	15.95	±	0.99	10.75	±	1.20	5.09	±	0.23	8.83	±	0.92	12.65	±	0.52	8.83	±	1.94
11	16	0.79	±	0.02	13.11	±	0.61	16.47	±	1.05	12.45	±	0.56	5.11	±	0.24	10.43	±	0.57	13.30	±	1.48	9.89	±	0.79
12	17	1.06	±	0.03	8.79	±	1.18	12.81	±	1.84	9.60	±	0.57	4.26	±	0.50	6.93	±	0.75	11.32	±	1.52	8.14	±	0.81
12	18	1.32	±	0.05	8.63	±	1.91	12.68	±	5.07	8.74	±	1.26	4.31	±	1.34	6.60	±	0.92	11.33	±	3.05	7.30	±	0.24
13	19	1.55	±	0.02	11.96	±	0.65	16.13	±	1.38	11.52	±	0.64	5.38	±	0.31	8.65	±	0.54	13.84	±	1.02	9.67	±	0.65
13	20	1.53	±	0.02	12.89	±	0.77	16.82	±	1.13	12.01	±	0.81	5.57	±	0.19	9.47	±	0.60	13.46	±	0.58	10.41	±	0.71
14	21	0.88	±	0.03	14.96	±	1.28	18.21	±	2.51	14.20	±	0.71	5.74	±	0.68	10.58	±	0.44	11.33	±	0.76	10.40	±	0.47
14	22	0.94	±	0.02	15.26	±	0.63	18.46	±	1.64	15.10	±	1.01	5.76	±	0.31	11.05	±	0.39	13.72	±	0.52	13.72	±	0.42

Figure 1

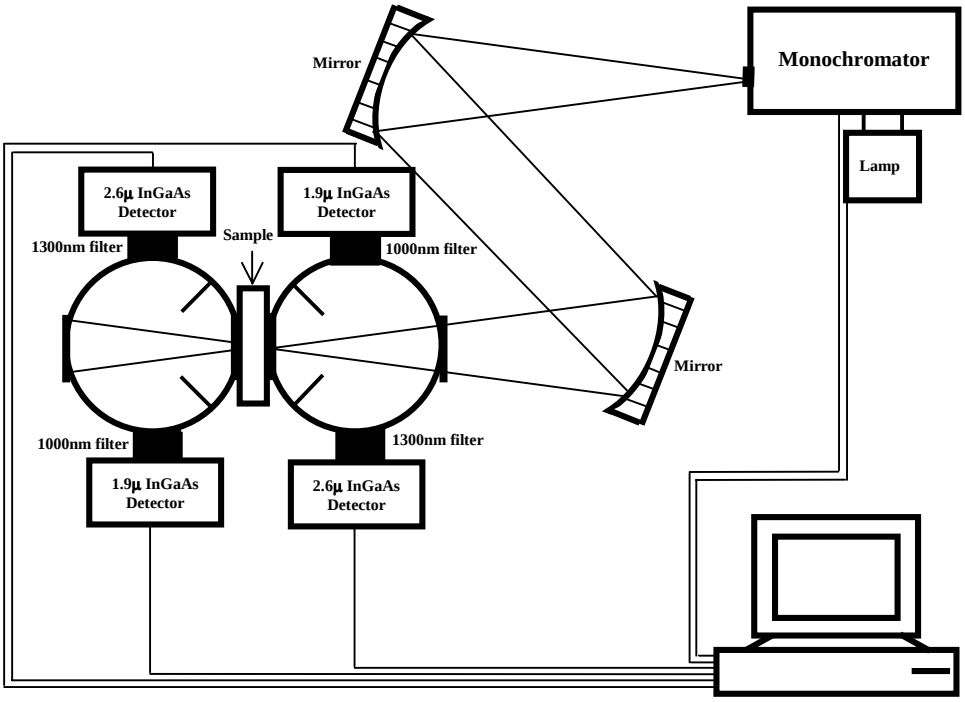
Mirror
Monochromator
Lamp
2.6μ InGaAs Detector
1.9μ InGaAs Detector
Sample
1300nm filter
1000nm filter
Mirror
1000nm filter
1300nm filter
1.9μ InGaAs Detector
2.6μ InGaAs Detector

Figure 2

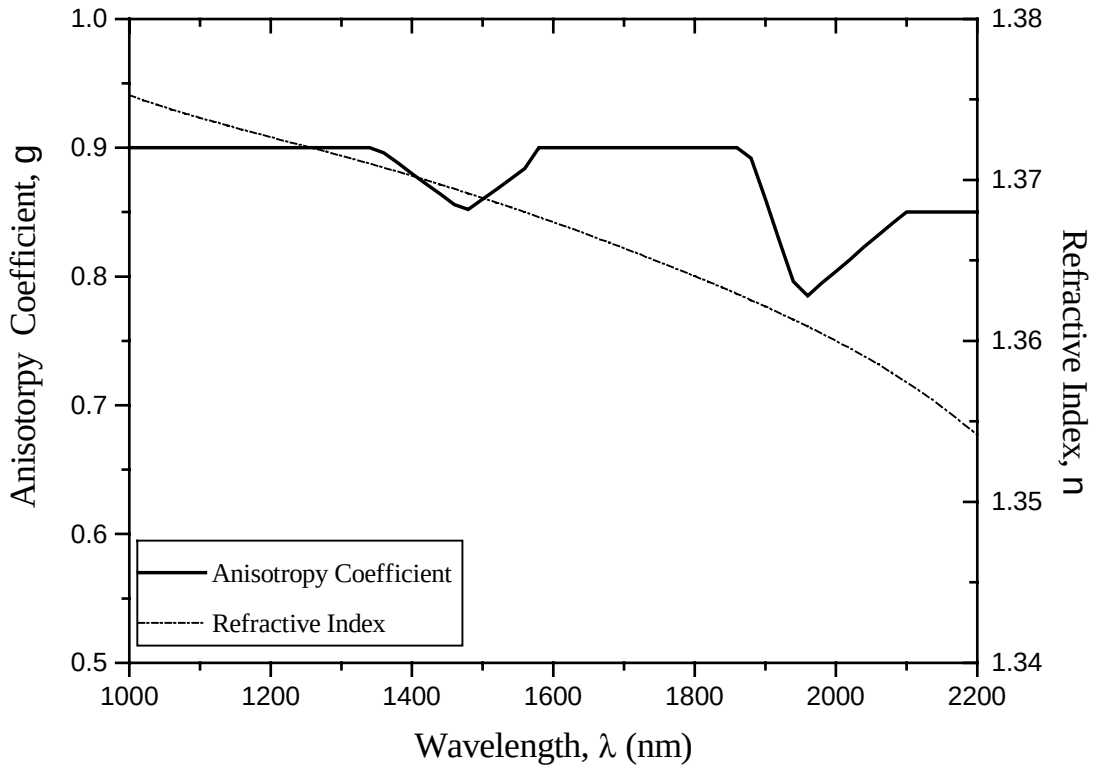
Anisotropy Coefficient, g
Refractive Index, n
Wavelength, λ (nm)
Anisotropy Coefficient
Refractive Index
1.0
0.9
0.8
0.7
0.6
0.5
1.38
1.37
1.36
1.35
1.34
1000
1200
1400
1600
1800
2000
2200

Figure 3

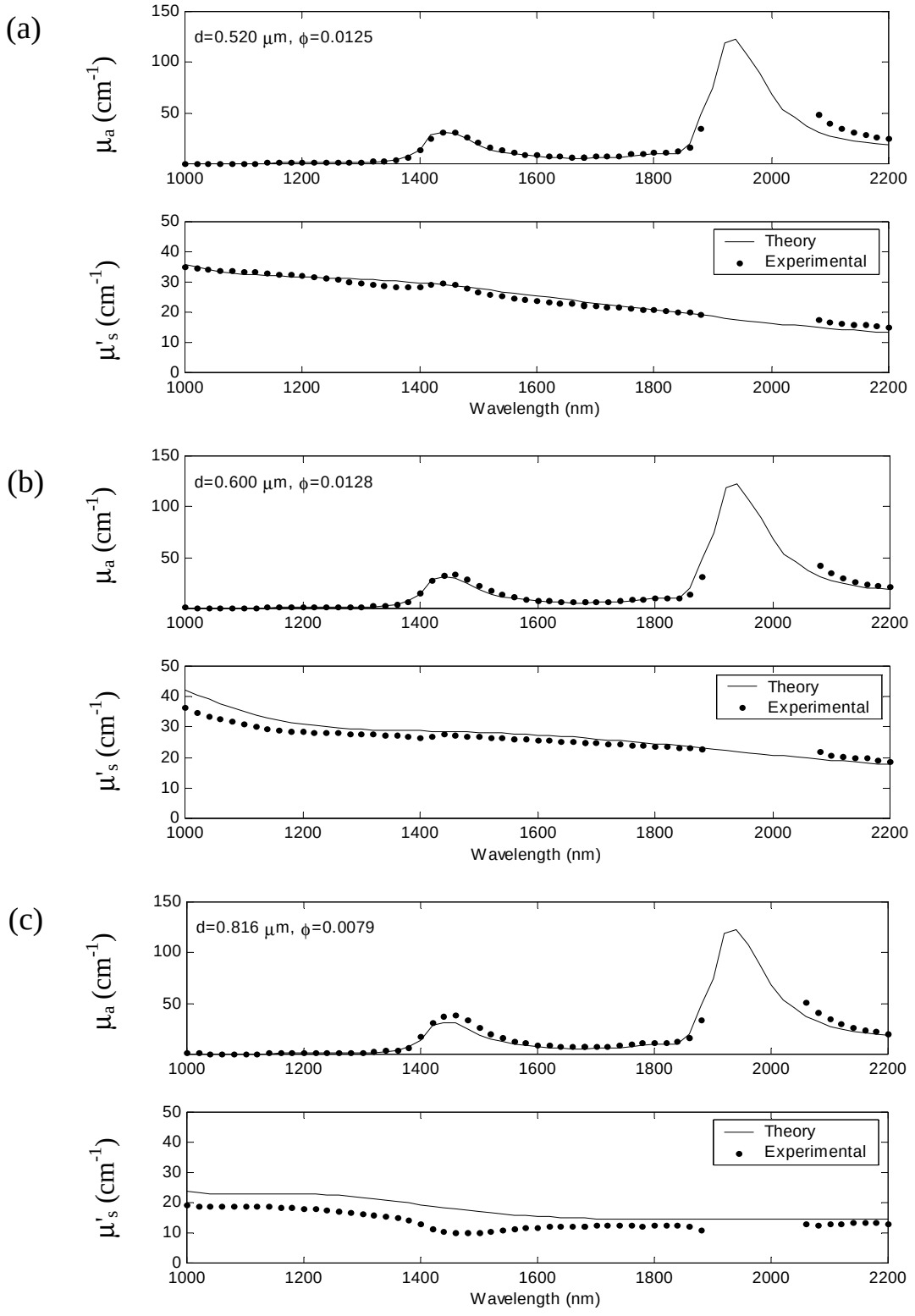
(a)
d=0.520 μm, ϕ=0.0125
μa (cm-1)
μ's (cm-1)
Theory
Experimental
(b)
d=0.600 μm, ϕ=0.0128
μa (cm-1)
μ's (cm-1)
Theory
Experimental
(c)
d=0.816 μm, ϕ=0.0079
μa (cm-1)
μ's (cm-1)
Theory
Experimental
Wavelength (nm)

Figure 4

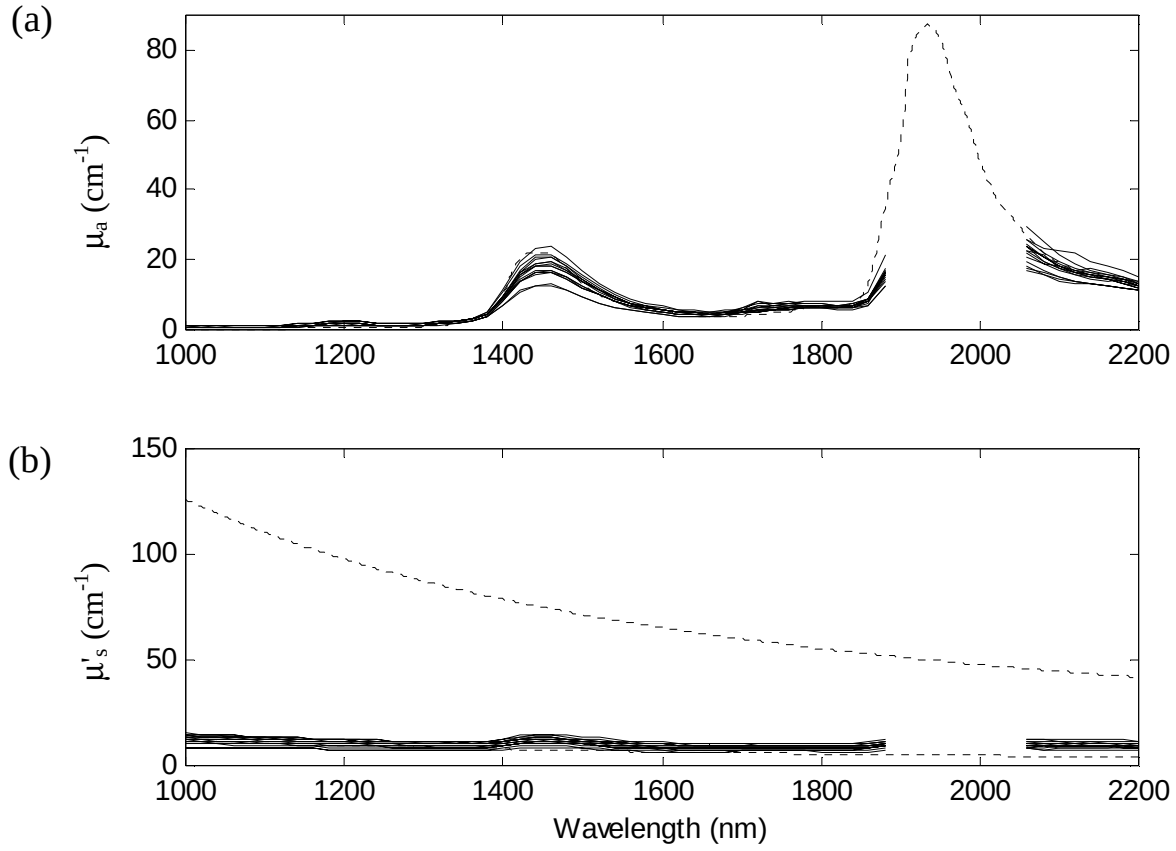
(a)
80
60
40
20
0
μ_a (cm^{-1})
1000
1200
1400
1600
1800
2000
2200
(b)
150
100
50
0
μ'_s (cm^{-1})
1000
1200
1400
1600
1800
2000
2200
Wavelength (nm)

Figure 5

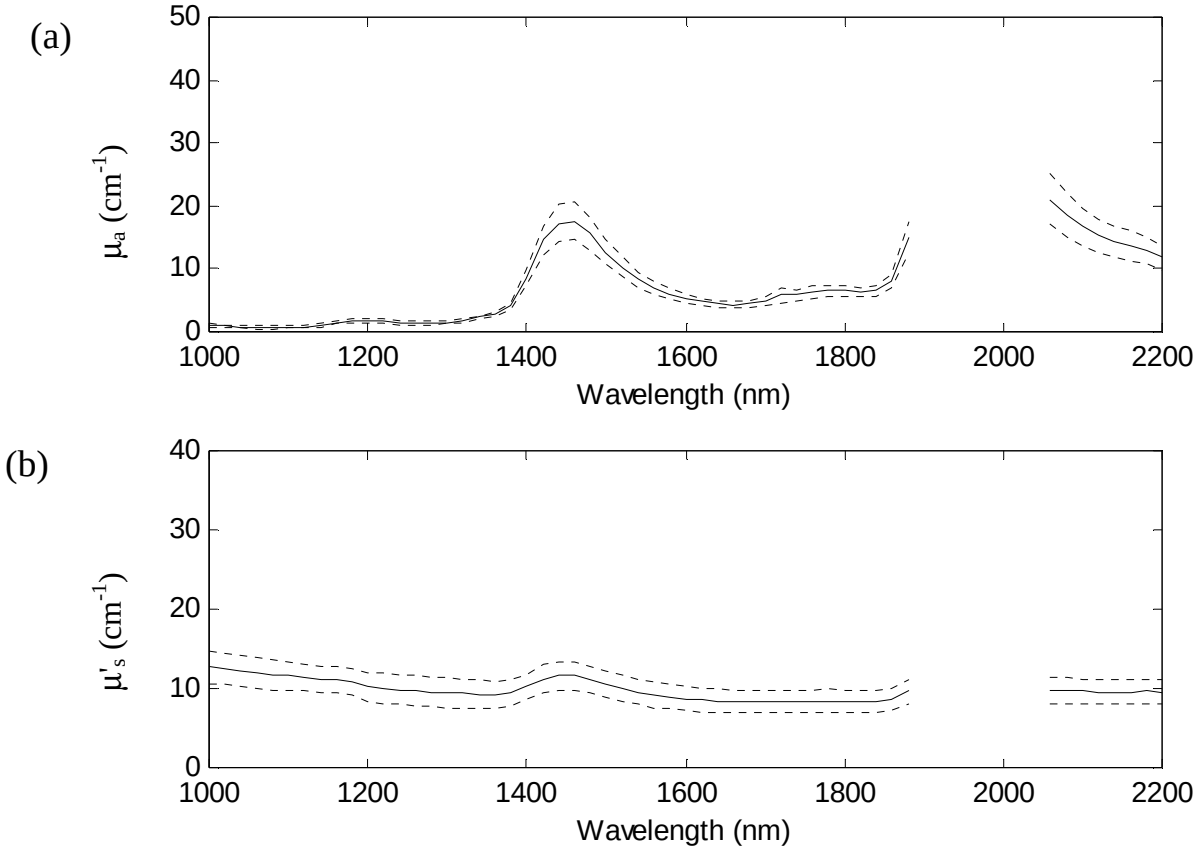
(a)
50
40
30
20
10
0
μ_a (cm^{-1})
1000
1200
1400
1600
1800
2000
2200
Wavelength (nm)
(b)
40
30
20
10
0
μ'_s (cm^{-1})
1000
1200
1400
1600
1800
2000
2200
Wavelength (nm)

Figure 6

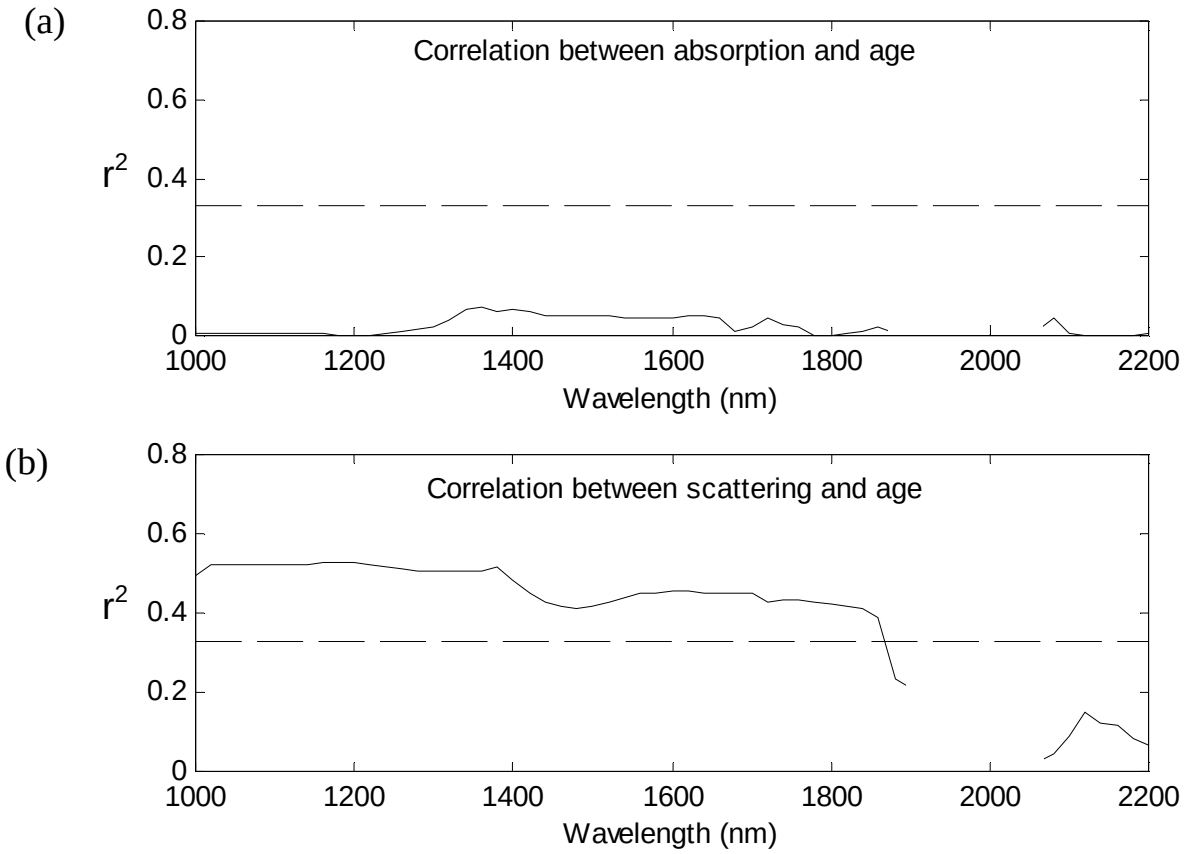
(a)
Correlation between absorption and age
r2
0.8
0.6
0.4
0.2
0
1000
1200
1400
1600
1800
2000
2200
Wavelength (nm)
(b)
Correlation between scattering and age
r2
0.8
0.6
0.4
0.2
0
1000
1200
1400
1600
1800
2000
2200
Wavelength (nm)

Figure 7

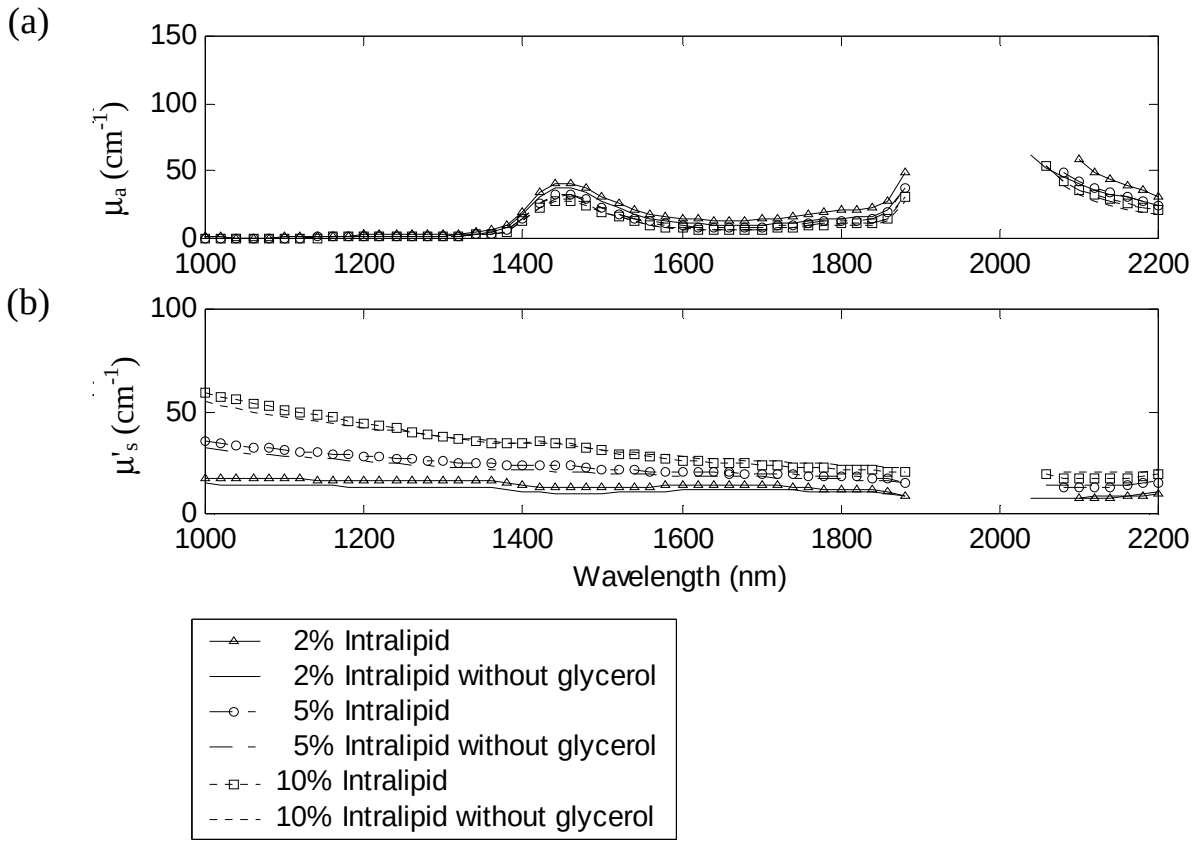
(a)
150
100
50
0
μ_a (cm^{-1})
1000
1200
1400
1600
1800
2000
2200
(b)
100
50
0
μ'_s (cm^{-1})
1000
1200
1400
1600
1800
2000
2200
Wavelength (nm)
2% Intralipid
2% Intralipid without glycerol
5% Intralipid
5% Intralipid without glycerol
10% Intralipid
10% Intralipid without glycerol

Figure 8

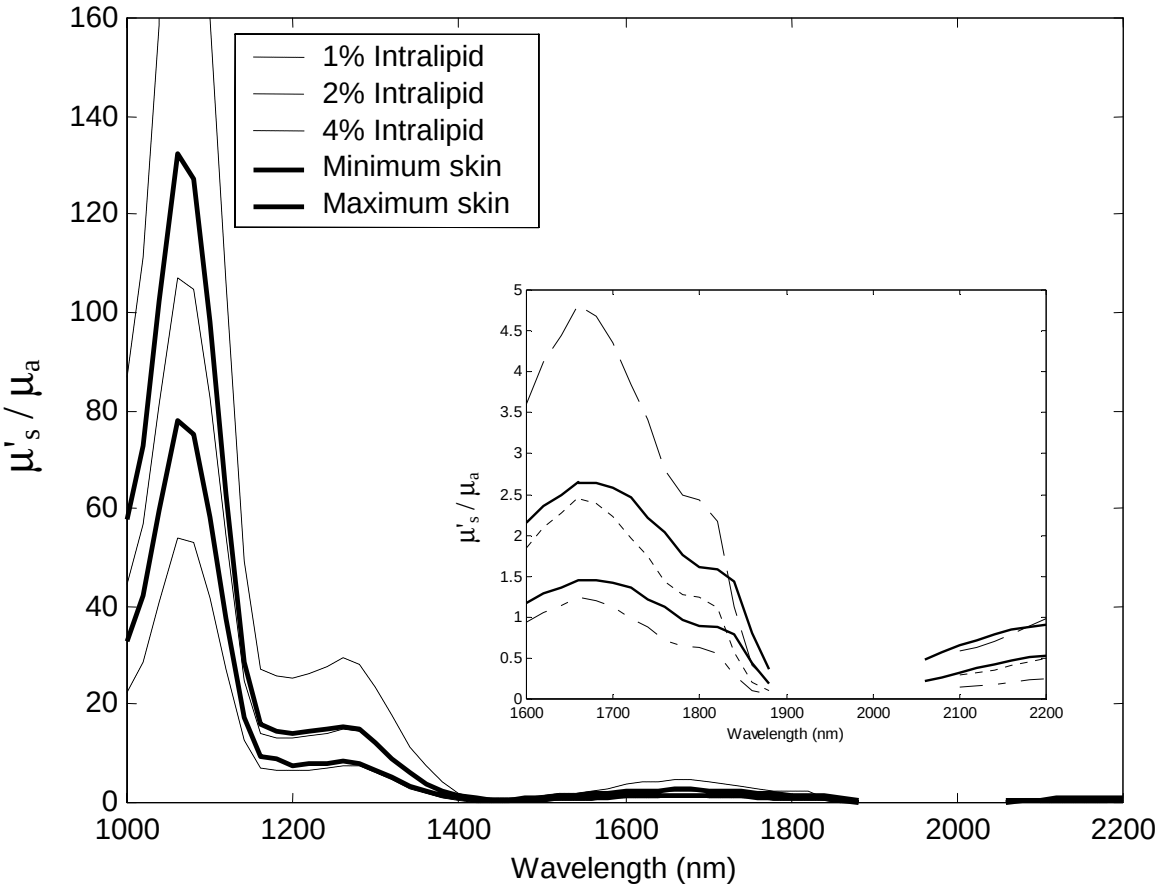
1% Intralipid
2% Intralipid
4% Intralipid
Minimum skin
Maximum skin
μ's / μa
Wavelength (nm)
160
140
120
100
80
60
40
20
0
1000
1200
1400
1600
1800
2000
2200
5
4.5
4
3.5
3
2.5
2
1.5
1
0.5
0
1600
1700
1800
1900
2000
2100
2200